Three-Dimensional Porous Coordination Polymer Functionalized with Amide Groups Based on Tridentate Ligand: Selective Sorption and Catalysis

Shinpei Hasegawa, Satoshi Horike, Ryotaro Matsuda, Shuhei Furukawa, Katsunori Mochizuki, Yoshinori Kinoshita, and Susumu Kitagawa*

Contribution from the Department of Synthetic Chemistry and Biological Chemistry, Graduate School of Engineering, Kyoto University, Katsura, Nishikyo-ku, Kyoto, 615-8510, Japan

Received October 14, 2006; E-mail: kitagawa@sbchem.kyoto-u.ac.jp

Abstract: To create a functionalized porous compound, amide group is used in porous framework to produce attractive interactions with guest molecules. To avoid hydrogen-bond formation between these amide groups our strategy was to build a three-dimensional (3D) coordination network using a tridentate amide ligand as the three-connector part. From $Cd(NO_3)_2 \cdot 4H_2O$ and a three-connector ligand with amide groups a 3D porous coordination polymer (PCP) based on octahedral Cd(II) centers, $\{[Cd(4\text{-btapa})_2(NO_3)_2] \cdot 6H_2O \cdot 2DMF\}_n$ (**1a**), was obtained (4-btapa = 1,3,5-benzene tricarboxylic acid tris[N-(4-pyridyl)amide]). The amide groups, which act as guest interaction sites, occur on the surfaces of channels with dimensions of 4.7×7.3 Å^2. X-ray powder diffraction measurements showed that the desolvated compound (**1b**) selectively includes guests with a concurrent flexible structural (amorphous-to-crystalline) transformation. The highly ordered amide groups in the channels play an important role in the interaction with the guest molecules, which was confirmed by thermogravimetric analysis, adsorption/desorption measurements, and X-ray crystallography. We also performed a Knoevenagel condensation reaction catalyzed by **1a** to demonstrate its selective heterogeneous base catalytic properties, which depend on the sizes of the reactants. The solid catalyst **1a** maintains its crystalline framework after the reaction and is easily recycled.

Introduction

In recent years, numerous studies of porous coordination polymers (PCPs), also called metal−organic frameworks (MOFs), have been reported[1] because of their applications in gas adsorption,[2] molecular storage,[3] and heterogeneous catalysis.[4] PCPs have characteristic features that include (1) well-ordered porous structures, (2) flexible and dynamic behaviors in response to guest molecules, and (3) designable channel surface functionalities. Although channel surface modification is essential for creation of functionalized porous structures, application of

this synthetic approach to the PCP system has received little attention. Two types of strategies are used to functionalize channel surfaces: immobilization of coordinatively unsaturated (open) metal sites (OMS)[5] and introduction of organic groups to provide guest-accessible functional organic sites (FOS).[4b,6] There is growing interest in the use of OMS for Lewis acid catalysis and specific gas adsorption, but less attention has been devoted to the study of FOS, despite their importance. The paucity of information on FOS is because of the difficulty of producing guest-accessible FOS on the pore surface: these

(1) (a) Yaghi, O. M.; Li, H.; Davis, C.; Richardson, D.; Groy, T. L. *Acc Chem. Res.* **1998**, *31*, 474−484. (b) Batten, S. R. *Curr. Opin. Solid State Mater. Sci.* **2001**, *5*, 107−114. (c) Moulton, B.; Zaworotko, M. J. *Chem. Rev.* **2001**, *101*, 1629−1658. (d) Janiak, C. *Dalton Trans.* **2003**, 2781−2804. (e) Kitagawa, S.; Kitaura, R.; Noro, S. *Angew. Chem., Int. Ed.* **2004**, *43*, 2334−2375. (f) Rosseinsky, M. J. *Microporous Mesoporous Mater.* **2004**, *73*, 15−30.

(2) (a) Eddaoudi, M.; Kim, J.; Rosi, N.; Vodak, D.; Wachter, J.; O'Keeffe, M.; Yaghi, O. M. *Science* **2002**, *295*, 469−472. (b) Kitaura, R.; Kitagawa, S.; Kubota, Y.; Kobayashi, T. C.; Kindo, K.; Mita, Y.; Matsuo, A.; Kobayashi, M.; Chang, H. C.; Ozawa, T. C.; Suzuki, M.; Sakata, M.; Takata, M. *Science* **2002**, *298*, 2358−2361. (c) Férey, G.; Latroche, M.; Serre, C.; Millange, F.; Loiseau, T.; Guégan, A. P. *Chem. Commun.* **2003**, 2976−2977. (d) Chu, H.; Dybtsev, D. N.; Kim, H.; Kim, K. *Chem. Eur. J.* **2005**, *11*, 3521−3529. (e) Rowsell, J. L. C.; Yaghi, O. M. *Angew. Chem., Int. Ed.* **2005**, *44*, 4670−4679. (f) Matsuda, R.; Kitaura, R.; Kitagawa, S.; Kubota, Y.; Belosludov, R. V.; Kobayashi, T. C.; Sakamoto, H.; Chiba, T.; Takata, M.; Kawazoe, Y.; Mita, Y. *Nature* **2005**, *436*, 238−241. (g) Dincă, M.; Long, J. R. *J. Am. Chem. Soc.* **2005**, *127*, 9376−9377.

(3) (a) Yaghi, O. M.; Li, H. *J. Am. Chem. Soc.* **1996**, *118*, 295−296. (b) Dalrymple, S. A.; Shimizu, G. K. H. *Chem. Eur. J.* **2002**, *8*, 3010−3015. (c) Kosal, M. E.; Chou, J. H.; Wilson, S. R.; Suslick, K. S. *Nat. Mater.* **2002**, *1*, 118−121. (d) Kim, H.; Suh, M. P. *Inorg. Chem.* **2005**, *44*, 810−812.

(4) (a) Fujita, M.; Kwon, Y. J.; Washizu, S.; Ogura, K. *J. Am. Chem. Soc.* **1994**, *116*, 1151−1152. (b) Seo, J. S.; Whang, D.; Lee, H.; Jun, S. I.; Oh, J.; Jeon, Y. J.; Kim, K. *Nature* **2000**, *404*, 982−986. (c) Wu, C. D.; Hu, A.; Zhang, L.; Lin, W. *J. Am. Chem. Soc.* **2005**, *127*, 8940−8941. (d) Lor, B. G.; Puebla, E. G.; Iglesias, M.; Monge, M. A.; Valero, C. R.; Snejko, N. *Chem. Mater.* **2005**, *17*, 2568−2573. (e) Sato, T.; Mori, W.; Kato, C. N.; Yanaoka, E.; Kuribayashi, T.; Ohtera, R.; Shiraishi, Y. *J. Catal.* **2005**, *232*, 186−198. (f) Dybtsev, D. N.; Nuzhdin, A. L.; Chun, H.; Bryliakov, K. P.; Talsi, E. P.; Fedin, V. P.; Kim, K. *Angew. Chem., Int. Ed.* **2006**, *45*, 916−920. (g) Uemura, T.; Kitaura, R.; Ohta, Y.; Nagaoka, M.; Kitagawa, S. *Angew. Chem., Int. Ed.* **2006**, *45*, 4112−4116.

(5) (a) Noro, S.; Kitagawa, S.; Yamashita, M.; Wada, T. *Chem. Commun.* **2002**, 222−223. (b) Kitaura, R.; Onoyama, G.; Sakamoto, H.; Matsuda, R.; Noro, S.; Kitagawa, S. *Angew. Chem., Int. Ed.* **2004**, *43*, 2684−2687. (c) Chen, B.; Fronczek, F. R.; Maverick, A. W. *Inorg. Chem.* **2004**, *43*, 8209−8211. (d) Maggard, P. A.; Yan, B.; Luo, J. *Angew. Chem., Int. Ed.* **2005**, *44*, 2−5. (e) Chen, B.; Ockwig, N. W.; Millward, A. R.; Contreras, D. S.; Yaghi, O. M. *Angew. Chem., Int. Ed.* **2005**, *44*, 4745−4749. (f) Cho, S. H.; Ma, B.; Nguyen, S. T.; Hupp, J. T.; Albrecht-Schmitt, T. E. *Chem. Commun.* **2006**, 2563−2565.

(6) (a) Kitaura, R.; Fujimoto, K.; Noro, S.; Kondo, M.; Kitagawa, S.; *Angew. Chem., Int. Ed.* **2002**, *41*, 133−135. (b) Shin, D. M.; Lee, I. S.; Chung, Y. K. *Inorg. Chem.* **2003**, *42*, 8838−8846. (c) Custelcean, R.; Gorbunova, M. G. *J. Am. Chem. Soc.* **2005**, *127*, 16362−16363.

Scheme 1. 1,3,5-Benzene Tricarboxylic Acid Tris[*N*-(4-pyridyl)amide] (4-btapa)
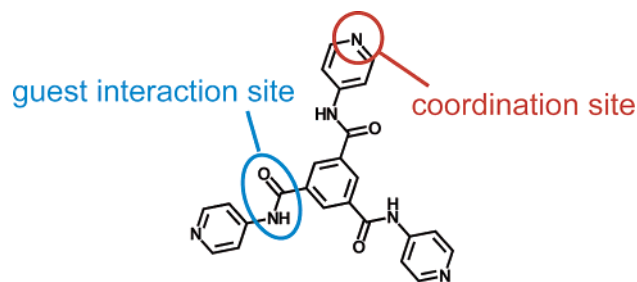
organic groups tend to coordinate metal ions via a self-assembly process, resulting in frameworks in which FOS are completely blocked.

The advantage of FOS is that the base-type catalyst is easy to create. There are a variety of organic functional groups that can serve as active base sites. In this report, we describe an approach for the preparation of a PCP using base-type FOS and demonstrate its base catalytic properties in a heterogeneous reaction. These observations will contribute to the development of new types of catalysts constructed from metal−organic frameworks.

PCPs with amide groups are candidate compounds that have FOS as guest interaction sites.[7] The amide group is a fascinating functional group because it possesses two types of hydrogen-bonding sites: the −NH moiety acts as an electron acceptor and the −C=O group acts as an electron donor.[8] These multifunctional moieties of amide groups tend to form hydrogen bonds among themselves and interact negligibly with guest molecules after construction of PCPs. If a PCP could be prepared without forming amide−amide interactions, these groups would constitute attractive interaction sites for selective sorption and/or catalysis inside the channel. To retain amide groups as guest-interaction FOS inside the network, we employed a three-connector ligand containing amide groups. Three-connector ligands are more useful for construction of 3D PCPs with coordination bonds than bidentate or monodentate ligands.[9] We employed a three-connector ligand containing three pyridyl groups as coordination sites and three amide groups as guest interaction sites (1,3,5-benzene tricarboxylic acid tris[*N*-(4-pyridyl)amide][10] (4-btapa, Scheme 1) and succeeded in producing a new base-type catalytic pore framework.

Experimental Section

General Information. 4-Aminopyridine and 1,3,5-benzene tricarboxylic acid trichloride were obtained from Tokyo Kasei Industrial. Cd(NO₃)₂·4H₂O was obtained from Wako without purification. Elemental analysis (EA) was carried out with a Thermo Finnigan EA1112. ¹H NMR spectra were measured in DMSO-d_6 with a (500 MHz) JEOL

JNM-A500 FT NMR system, and chemical shifts are reported in δ (ppm) values. Solid-state magic angle spinning/cross polarization (CPMAS) ¹¹³Cd NMR experiment was carried out on a (300 MHz) JEOL JNM-LA300WB spectrometer. IR spectra were recorded on a Perkin-Elmer 2000 FT−IR spectrophotometer with samples prepared with KBr pellets. Thermogravimetric analyses (TGA) were performed using a Rigaku Thermo plus TG 8120 apparatus in the temperature range between 298 and 723 K in a N₂ atmosphere and at a heating rate of 10 K min⁻¹. X-ray powder diffraction (XRPD) data were collected on a Rigaku RINT-2200HF (Ultima) diffractometer with Cu Kα radiation. The adsorption isotherm of nitrogen at 77 K and methanol at 298 K were measured with BELSORP18 volumetric adsorption equipment from Bel Japan, Inc.

Ligand (4-btapa). A solution of 4-aminopyridine (17.0 g, 180 mmol) and distilled triethylamine (27 mL, 194 mmol) in distilled THF (200 mL) was added dropwise to a solution of 1,3,5-benzene tricarboxy-trichloride (16.1 g, 60.0 mmol) in THF (60 mL) at 0 °C. Triethylamine (9.0 mL, 65 mmol) was added, and the reaction mixture was stirred for 7 h. The temperature was allowed to step up to room temperature. The brown crude product of 4-btapa was collected by filtration and washed with THF. The product was recrystallized from DMSO (700 mL) and H₂O (1500 mL) by stirring for 1 h. The product was washed with acetone (1000 mL) by stirring for 1 day. The yellowish white powder was collected by filtration, washed with acetone, and dried under vacuum for 35 h at room temperature (21.4 g, 81%). ¹H NMR (500 MHz, DMSO-d_6): δ 10.95 (s, 3H, NH), 8.75 (s, 3H, −H$_{2,4,6}$-ph), 8.52 (d, 6H, J_{H-H} = 5.0 Hz, H$_{3,5}$-py), 7.82 (d, 6H, J_{H-H} = 5.0 Hz, H$_{2,6}$-py). FAB-MS (*m/z*): calcd for C₂₄H₁₈N₆O₃, 438.14; found, 438. Anal. Calcd for C₂₄H₁₈N₆O₃ (438.5): C, 65.75; H, 4.14; N, 19.17. Found: C, 64.84; H, 4.05; N, 18.81.

{[Cd(4-btapa)₂(NO₃)₂]·6H₂O·2DMF}ₙ (1a). A solution of Cd-(NO₃)₂·4H₂O (9.3 mg, 0.030 mmol) in MeCN (1.5 mL) was carefully layered on a solution of in 4-btapa (20 mg, 0.045 mmol) in DMF (1.5 mL) with MeCN/DMF (0.75 mL/0.75 mL) placed between the two layers. Colorless single crystals began to form in a few days. One of these crystals was used for X-ray crystallographic analysis. The bulk product was obtained by the following procedure. A solution of Cd-(NO₃)₂·4H₂O (0.93 g, 3.0 mmol) in DMF (50 mL) was added to a solution of 4-btapa (2.0 g, 4.5 mmol) in DMF (50 mL). The reaction mixture was stirred for 3.5 h. The crystalline yellowish white powder **1a** was obtained by filtration, washed with DMF, and dried under vacuum for 1 day at room temperature (2.86 g, 93% yield based on 4-btapa). Anal. Calcd for {[Cd(4-btapa)₂(NO₃)₂]·6H₂O·2DMF}ₙ (**1a**) C₅₄H₆₂CdN₁₆O₂₀ (1367.58): C, 47.42; H, 4.57; N, 16.39. Found for single crystal: C, 48.23; H, 4.66; N, 16.75. Found for bulk product: C, 48.29; H, 4.30; N, 16.52. For X-ray crystallographic analysis some guest molecules that show positional disorder could not be fixed in the structure model like the early compounds.[5b,11] The formula {[Cd-(4-btapa)₂(NO₃)₂]·6H₂O·2DMF}ₙ (**1a**) was assigned by EA, TGA, ¹H NMR, IR, as well as single-crystal X-ray diffraction studies.[12] Further details of experimental studies are given in the Supporting Information.

{[Cd(4-btapa)₂]·2NO₃}ₙ (1b). The amorphous yellowish white powder **1b** was obtained by drying **1a** under vacuum for 7.5 h at 140 °C. Removal of all solvent molecules was checked by TGA. The amorphous state of **1b** was checked by XRPD. Anal. Calcd for [Cd-

(7) (a) Uemura, K.; Kitagawa, S.; Kondo, M.; Fukui, K.; Kitaura, R.; Chang, H. C.; Mizutani, T. *Chem. Eur. J.* **2002**, *8*, 3586−3600. (b) Uemura, K.; Kitagawa, S.; Fukui, K.; Saito, K. *J. Am. Chem. Soc.* **2004**, *126*, 3817−3828. (c) Tzeng, B. C.; Chen, B. S.; Yeh, H. T.; Lee, G. H.; Peng, S. M. *New J. Chem.* **2006**, *30*, 1087−1092.

(8) (a) Lee, C. M.; Kumler, W. D. *J. Am. Chem. Soc.* **1962**, *84*, 571−578. (b) Bent, H. A. *Chem. Rev.* **1968**, *68*, 587−648. (c) Huyskens, P. L. *J. Am. Chem. Soc.* **1977**, *99*, 2578−2582.

(9) (a) Batten, S. R.; Murray, K. S. *Coord. Chem. Rev.* **2003**, *246*, 103−130. (b) Chae, H. K.; Siberio-pérez, D. Y.; Kim, J.; Go, Y.; Eddaoudi, M.; Matzger, A. J.; O'Keeffe, M.; Yaghi, O. M. *Nature* **2004**, *427*, 523−527. (c) Ohmori, O.; Kawano, M.; Fujita, M. *J. Am. Chem. Soc.* **2004**, *126*, 16292−16293.

(10) Kumar, D. K.; Jose, D. A.; Dastidar, P.; Das, A. *Chem. Mater.* **2004**, *16*, 2332−2335.

(11) (a) Hoskins, B. F.; Robson, R. *J. Am. Chem. Soc.* **1989**, *111*, 5962−5964. (b) Ohmori, O.; Fujita, M. *Chem. Commun.* **2004**, 1586−1587. (c) Luo, T. T.; Tsai, H. L.; Yang, S. L.; Liu, Y. H.; Yadav, R. D.; Su, C. C.; Ueng, C. H.; Lin, L. G.; Lu, K. L. *Angew. Chem., Int. Ed.* **2005**, *44*, 6063−6067.

(12) Some guest molecules that show positional disorder could not be fixed in the structure model. During the final stages of refinement, several Q peaks were found, which probably correspond to highly disordered molecules. However, each guest molecule was detected by EA, TGA, IR, and ¹H NMR. Crystal data for **1a**: C₄₈H₃₆CdN₁₂O₁₂, M_r = 1085.30, cubic, *Ia-3* (#206), a = 24.756(4) Å, V = 15171.6(43) Å³, Z = 8, $F(000)$ = 4423.68, ρ_{calcd} = 0.952 gcm⁻³, μ = 0.342 mm⁻¹, GOF = 0.904. A total of 84 868 reflections were collected in the range 2θ = 6.2−55.0°, of which 2896 were unique. Final $R1$ and $wR2$ are 0.080 and 0.216, respectively, for 112 parameters and 1350 reflections [$I > 3\sigma(I)$].
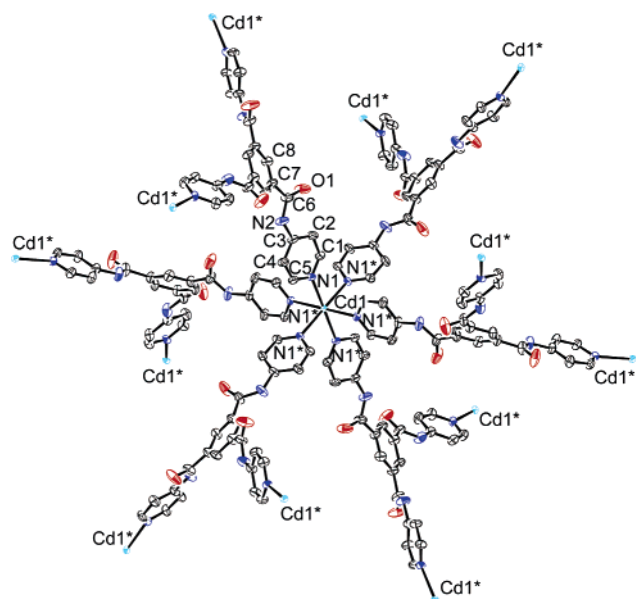
Figure 1. ORTEP drawing of **1a** with ellipsoids probability 30% (asterisk indicates atoms that are symmetrically related). Cd(II) centers are octahedrally coordinated to N atoms of different six 4-btapa. H₂O molecules and hydrogen atoms are omitted for clarity.

(4-btapa)₂(NO₃)₂] (**1b**) (1113.30): C, 51.78; H, 3.26; N, 17.61. Found for bulk product: C, 49.52; H, 3.57; N, 16.66.

{[Cd(4-btapa)₂(NO₃)₂]·6MeOH·yH₂O}ₙ (1c). The methanol-exchanged colorless compound **1c** was obtained by exposing **1b** on the methanol vapor for 30 h at room temperature. The amount of adsorbed methanol molecules was checked by TGA and ¹H NMR.

X-ray Structure Determination. The colorless single crystal of **1a** was mounted on glass fibers with epoxy resin. X-ray data collection for the single crystal was carried out on a Rigaku Mercury diffractometer with graphite-monochromated Mo Kα radiation ($\lambda = 0.71070$ Å) and a CCD two-dimensional detector at 238 K in a cold nitrogen stream. The X-ray condition for **1a** was 50 kV × 40 mA. The structure was solved by direct method using the SHELXS-97 program and refined by the full-matrix least-squares method on F^2 with appropriate software implemented in the crystals program package. The final cycles of the full-matrix least-squares refinements were based on the observed reflections [$I > 3\sigma(I)$]. All calculations were performed using the crystal structure program package. All non-hydrogen atoms except for those of disordered solvent molecules in **1a** were refined anisotropically. Hydrogen atoms were added at their geometrically ideal positions and refined isotropically. Further refinement was unsuccessful because counteranions and some solvent molecules were highly disordered, and the high symmetric position in **1a** would make occupancies of these atoms decrease.

Selective Accommodation and Activation of Reactants. For each reagent (malononitrile, ethyl cyanoacetate, and cyano-acetic acid *tert*-butyl ester), the accommodation procedure was carried out. The as-synthesized **1a** (0.10 g) and a reagent (2 mmol) in dehydrated benzene (10 mL) were stirred for 6 h. The precipitates were filtrated and dried in the open air for 1.5 h and then identified by IR (KBr pellet) and ¹H NMR (DMSO-d_6) spectroscopies.

Knoevengael Condensation Reaction Catalyzed by 1a. A solution of benzaldehyde (0.21 mL, 2.1 mmol) and malononitrile (or ethyl cyanoacetate or cyano-acetic acid *tert*-butyl ester) (0.132 g, 2.0 mmol) in benzene (10 mL) was stirred for 5 min. Then **1a** (0.10 g, 0.08 mmol, 4 mol %) was added. The suspension was stirred at room temperature for 12 h. The progress of the reaction was monitored by ¹H NMR (DMSO-d_6). The catalyst was removed by filtration, washed with benzene, and recovered.
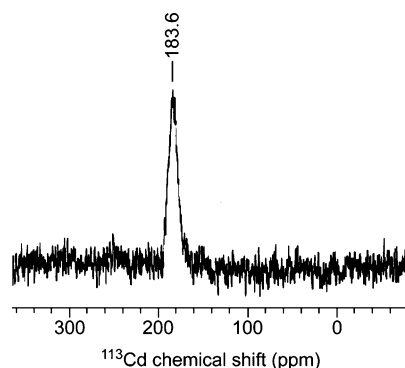
Figure 2. Solid-state ¹¹³Cd CPMAS NMR spectrum of **1a** at a MAS spinning rate of 4382 Hz.

Table 1. Selected Bond Distances (Å) and Angles (deg) for {[Cd(4-btapa)₂(NO₃)₂]·6H₂O·2DMF}ₙ (**1a**)[a]

Cd (1)−N1	2.372 (7)	Cd1−N1¹	2.372 (8)
Cd1−N1²	2.372 (8)	Cd1−N1³	2.372 (8)
Cd1−N1⁴	2.372 (8)	Cd1−N1⁵	2.372 (7)
N1¹−Cd1−N1	90.8 (3)	N1²−Cd1−N1	90.8 (3)
N1³−Cd1−N1		N1⁴−Cd1−N1	89.2 (3)
N1⁵−Cd1−N1		N1²−Cd1−N1¹	90.8 (3)
N1³−Cd1−N1¹	89.2 (3)	N4⁴−Cd1−N4¹	89.2 (3)
N1⁵−Cd1−N1¹	180.0 (4)	N1³−Cd1−N1²	89.2 (3)
N1⁴−Cd1−N1²	180.0 (4)	N1⁵−Cd1−N1²	89.2 (3)
N1⁴−Cd1−N1³	90.8 (3)	N1⁵−Cd1−N1³	90.8 (3)
N1⁵−Cd1−N1⁴	90.8 (3)		

[a] Symmetry transformation used to generate equivalent atoms: 1 = (y, z, x); 2 = (z, x, y); 3 = (−y, −z, −x); 4 = (−z, −x, −y); 5 = (−x, −y, −z); 6 = (−z + 1/2, −x, y + 1/2).

Results and Discussion

Structural Description. The coordination environment around Cd(II) of {[Cd(4-btapa)₂(NO₃)₂]·6H₂O·2DMF}ₙ (**1a**) is shown in Figure 1. The Cd(II) center is octahedrally coordinated to six pyridyl nitrogen atoms from different bridging (4-btapa) connectors. To the best of our knowledge, **1a** is the first compound in which Cd(II) is coordinated to six pyridyl groups as the ideal octahedral coordination environment. All the Cd−N bond lengths and angles are similar to each other (Table 1). The solid-state cross-polarization magic-angle spinning (CP-MAS) ¹¹³Cd nuclear magnetic resonance (NMR) spectrum for **1a** also supports the ideal octahedral coordination environment of Cd(II). The spectrum has one resonance centered at 183.6 ppm (Figure 2). It is well known that each aromatic nitrogen donor ligand in the CdN₄ plane contributes approximately +50 ppm.[13] Therefore, in this compound the chemical shift should have a value of ca. +200 ppm directed normal to the 4N plane. The observed value of 183.6 ppm is in agreement with this value. Furthermore, one can safely state that the one single resonance peak indicates a highly symmetrical coordination environment around the Cd(II) center.

3-D Porous Framework Functionalized with Amide Groups. The framework of **1a** was constructed from the Cd(II) center as a six-connected node using 4-btapa as a three-connected linker. This arrangement produces a large six-membered ring composed of three octahedral Cd(II) moieties linked together by three 4-btapa units. The six-membered ring is distorted because of the rotation of 4-btapa between the benzene ring and the amide group (Figure 3a). The framework expands in

(13) Griffith, E. A. H.; Li, H. Y.; Amma, E. L. *Inorg. Chim. Acta* **1988**, *148*, 203−208.
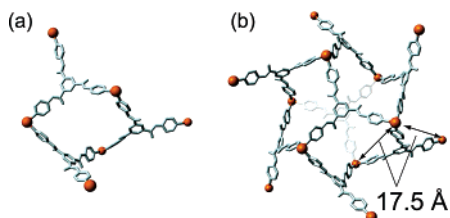
Figure 3. Crystal structure of $\{[Cd(4\text{-btapa})_2(NO_3)_2]\cdot 6H_2O\cdot 2DMF\}_n$ (**1a**). (a) The distorted 6-membered ring composed of three octahedral Cd(II) linked together by three 4-btapa units. (b) The framework expanding three directions to form a 3-D framework. Orange and sky blue represent Cd(II) and the framework. H atoms and guests are omitted for clarity.
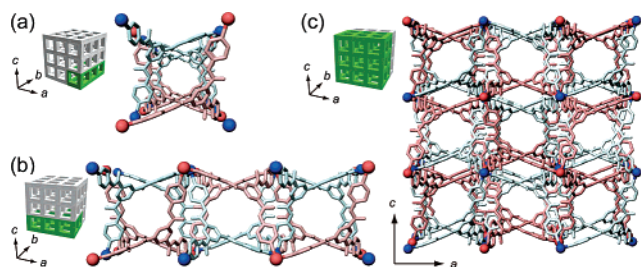
Figure 4. (a−c) Two-fold interpenetrating 3-D crystal structure of **1a** to form three-dimensionally running channels of dimensions 4.7×7.3 Å.[2] The perspective view is down from the *b* axis. Guests and H atoms are omitted for clarity.
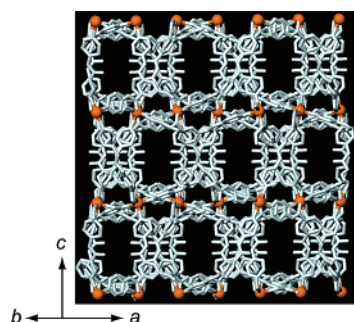

Figure 5. Crystal structure of **1a** to form another type of zigzag channels with dimensions of 3.3×3.6 Å.[2] Guests and H atoms are omitted for clarity.

three directions, with a Cd(II)···Cd(II) separation of 17.5 Å, to form a 3D network (Figure 3b). The two frameworks mutually interpenetrate with a nearest-neighbor Cd(II)···Cd(II) distance of 12.4 Å between Cd(II) atoms in the adjacent frameworks, producing three-dimensionally running channels (so-called 3D pores) with dimensions of 4.7×7.3 Å,[2] which are available for guest accommodation and exchange (Figure 4). The channel is not straight but zigzags and occupied by nitrate anions and H_2O and DMF molecules. Two nitrate anions, six H_2O molecules, and two DMF molecules per formula unit have been confirmed by elemental analysis (EA), thermogravimetric analysis (TGA), infrared spectroscopy (IR), and ^1H NMR,[14] in addition to the crystallographic results. **1a** also has another type of zigzag channel, with dimensions of 3.3×3.6 Å,[2] running in three directions (Figure 5). In **1a**, 43.8% of the void space is accessible to the solvent molecules.[15,16] The nearest N(amide)-

(14) More detailed measurement results are available in the Supporting Information.

(15) The void space was calculated by PLATON.[16] The value was taking the volume of NO_3^- (77.0 Å[3]) into account. The size is calculated by considering van der Waals radii for NO_3^- molecules. The value is in the following reference. Israelachvili, J. N. *Intermolecular and surface forces*, 2nd ed.; Academic Press: New York, 1992.
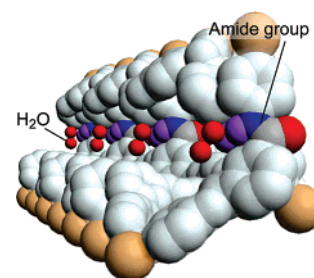
Figure 6. View of the ordered amide groups on the channel surface. H_2O molecules are interacted by hydrogen bonds with the NH group of the amide groups. Light brown, red, blue, gray, and purple represent channel surface, Cd(II), O, N, C, and H, respectively.
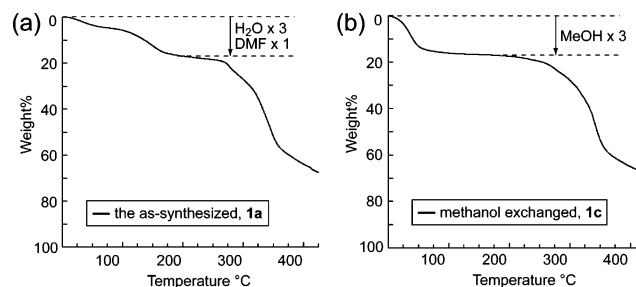

Figure 7. Thermogravimetric analyses of (a) **1a** and (b) **1c** over the temperature range from 25 to 450 °C at a heating rate of 10 °C min^{-1} under N_2 atmosphere. Amount of guests in figures is based on one 4-btapa ligand of each compound.

to-N(amide) distances are about 24.8 Å in the network and 4.0 Å between the two adjacent networks. The distance of N(amide)-to-O(amide) is about 9.7 Å. Consequently, the amide groups, which are highly ordered on the surfaces of the channels, could interact with guest molecules. The X-ray crystallographic results clearly show that H_2O molecules interact weakly via hydrogen bonds with the NH moieties of all the amide groups (O[water]···N[amide] = ca. 3.1 Å) (Figure 6). The amide groups inside the pores would act as important FOS in the interaction between the host and guest molecules.

Thermogravimetric Analyses of 1a and 1c. As seen in the crystal structure analysis and ^1H NMR results, **1a** includes H_2O and DMF molecules as guests. The desorption process was monitored by TGA. The observed weight loss of the guest molecules is in agreement with that calculated for the corresponding crystal structure. The TGA data for **1a** are indicative of two stages of weight loss for the guest molecules: six H_2O molecules and two DMF molecules per formula unit (Figure 7a). The resultant species, $[Cd(4\text{-btapa})_2(NO_3)_2]_n$ (**1b**), is stable up to 250 °C and then gradually decomposes with the loss of 4-btapa. The TGA curve showed that the weight loss below 150 °C of the methanol-exchanged compound **1c** corresponds to three methanol molecules per 4-btapa ligands (Figure 7b). The amount of methanol adsorbed is in good agreement with the number of amide groups in the host framework.

Recoverable Collapse on Desolvation and Resolvation. 1a, 1b, and **1c** are insoluble in water or common organic solvents and only soluble in dimethyl sulfoxide. Removal of the guest molecules causes a significant structural change in the framework of **1a**. As-synthesized crystalline **1a** changes to the amorphous state **1b** after heating under reduced pressure. The

(16) Spek, A. L. *PLATON, a multipurpose crystallographic tool*; Utrecht University: Utrecht, The Netherlands, 2001.
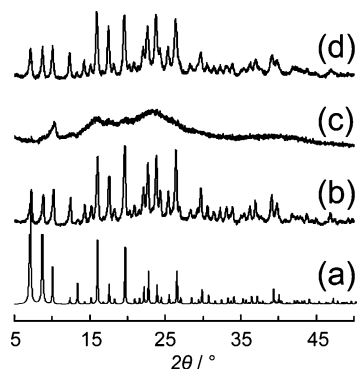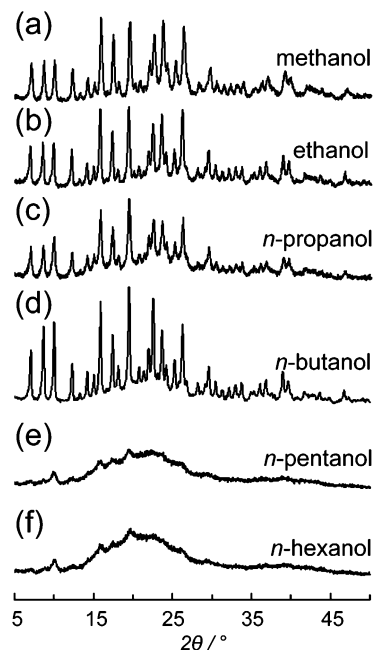
Figure 8. XRPD patterns of (a) **1a** simulation based on the single-crystal structure, (b) the as-synthesized **1a**, (c) the desolvated compound **1b**, which is obtained from **1a** under vacuum for 7.5 h at 140 °C, and (d) the methanol-exchanged compound **1c** obtained by exposing **1b** to methanol vapor for 30 h.

X-ray powder diffraction (XRPD) patterns for **1a** and **1b** are shown in Figure 8. This crystalline-to-amorphous transformation is accompanied by loss of the H$_2$O and DMF guest molecules in the channels, and the structural behavior has also been observed in other compounds.[17] However, when amorphous **1b** is immersed in methanol or exposed to methanol vapor, it changes immediately to the original crystalline phase (**1c**), which was detected by XRPD (Figure 8). We can rule out the possibility of recrystallization because of the low solubility and the results of experiments on vapor exposure. The amorphous-to-crystalline transformation is also induced by H$_2$O or DMF.[18] These types of flexible frameworks provide pore structures that are suitable for given guest molecules and much more useful for molecular recognition or selective guest inclusion than are robust porous structures.[19]

Selective Binding of Alcohols Inspired by Hydrogen Bonding. The desolvated host **1b** can easily include certain alcohols via hydrogen bonding with the amide groups. **1b** was immersed in a few drops of various alcohols, and the XRPD was measured; several of these experiments are shown in Figure 9. Short-chain alcohols (methanol, ethanol, *n*-propanol, and *n*-butanol) exhibited guest inclusion with structural transformation. Conversely, long-chain alcohols (*n*-pentanol and *n*-hexanol) caused no change in the XRPD patterns, indicating that **1b** did not undergo a structural change with guest adsorption. This selective inclusion system reflects the size of the guest molecule.

1b also exhibits unique selectivity responsive to functional groups of guests. Figure 10 shows the XRPD patterns of **1b** that was immersed in *n*-butanol, *n*-pentane, or *n*-pentene. Unlike its response to *n*-pentane and *n*-pentene, which have no OH groups, **1b** immersed in *n*-butanol exhibited guest inclusion with structural transformation. Considering the fact that *n*-butanol, *n*-pentane, and *n*-pentene are similar in size and shape, this selective inclusion system reflects the presence/absence, in the guest, of OH groups that would be available for hydrogen bonding. On the other hand, in IR spectra for **1a**, **1b**, and **1a**

(17) (a) Maspoch, D.; Ruiz-Molina, D.; Wurst, K.; Domingo, N.; Cavallini, M.; Biscarini, F.; Tejada, J.; Rovira, C.; Veciana, J. *Nat. Mater.* **2003**, *2*, 190−195. (b) Carlucci, L.; Ciani, G.; Moret, M.; Proserpio, D. M.; Rizzato, S. *Angew. Chem., Int. Ed.,* **2000**, *39*, 1506−1510.
(18) The XRPD patterns are shown in Figures S3 and S4.
(19) (a) Lee, E. Y.; Jang, S. Y.; Suh, M. P. *J. Am. Chem. Soc.* **2005**, *127*, 6374−6381. (b) Maji, T. K.; Mostafa, G.; Matsuda, R.; Kitagawa, S. *J. Am. Chem. Soc.* **2005**, *127*, 17152−17153. (c) Kitagawa, S.; Uemura, K. *Chem. Soc. Rev.* **2005**, *34*, 109−119. (d) Uemura, K.; Matsuda, R.; Kitagawa, S. *J. Solid State Chem.* **2005**, *178*, 2420−2429.

Figure 9. XRPD patterns for desolvated compound **1b** immersed in a few drops of (a) methanol, (b) ethanol, (c) *n*-propanol, (d) *n*-butanol, (e) *n*-pentanol, and (f) *n*-hexanol solution.
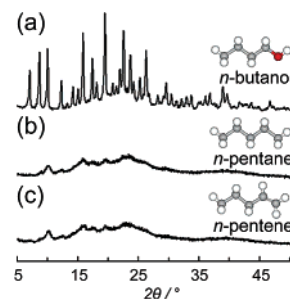

Figure 10. XRPD patterns for desolvated compound **1b** immersed in a few drops of (a) *n*-butanol, (b) *n*-pentane, and (c) *n*-pentene solution.

with other guests, the NO symmetric stretching vibration band of NO$_3^-$ can be seen at 1385 cm^{-1} (Figure S1), supporting no coordination or strong interaction of nitrate anions with the amide moieties in the framework.[20] In the case of the chloride derivative of **1b**, the Cl$^-$ ions clearly interact with the amide moieties inside the channels, resulting in no porous properties such as sorption or catalysis.[7c] Therefore, weaker participation of anions such as NO$_3^-$ in this study might be important for successful formation of functional PCP system with the amide groups.

Gas Sorption Properties with Dynamic Structural Transformation. The mechanism of guest binding, with structural transformation, should be investigated in detail. The adsorption and desorption behaviors of some guests were examined. **1b** showed no N$_2$ adsorption at 77 K, as shown in Figure 11. This result indicates that **1b** does not retain channels available for N$_2$ (kinetic diameter = 3.64 Å).[21] Because **1b** undergoes an amorphous-to-crystalline transformation when exposed to methanol vapor, methanol adsorption and desorption experiments were carried out on **1b**. The adsorption and desorption isotherms for
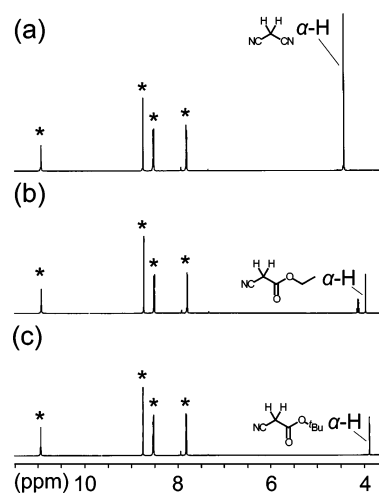
(20) (a) Newman, S. P.; Jones, W. *J. Solid State Chem.* **1999**, *148*, 26−40. (b) Xu, Z. P.; Zeng, H. C. *J. Phys. Chem. B* **2001**, *105*, 1743−1749.
(21) Pan, L.; Adams, K. M.; Hernandez, H. E.; Wang, X.; Zheng, C.; Hattori, Y.; Kaneko, K. *J. Am. Chem. Soc.* **2003**, *125*, 3062−3067.
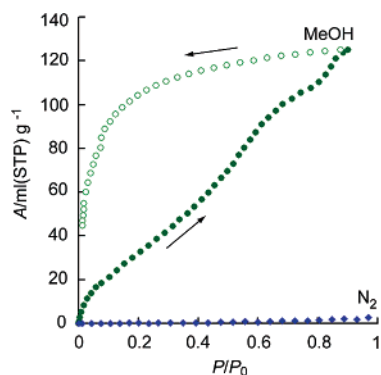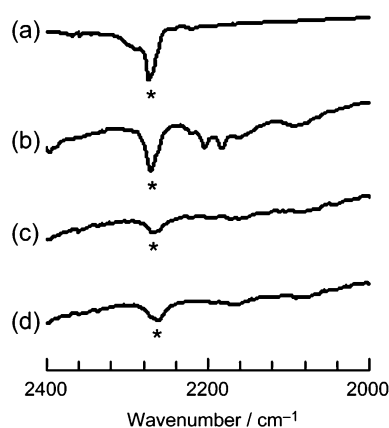
Figure 11. Gas adsorption/desorption isotherms for the uptake of N$_2$, MeOH. P_0 is the saturated vapor pressure, 102.3 kPa, of N$_2$ (77 K), and 16.94 kPa, of methanol (298 K).

Figure 12. ^{1}H NMR (DMSO-d_6) spectra of **1a** that adsorbed each guest molecule: (a) malononitrile, (b) ethyl cyanoacetate, and (c) cyano-acetic acid *tert*-butyl ester. The peaks marked with an asterisk indicate the 4-btapa.
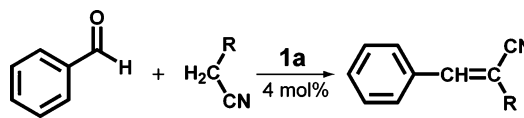

Figure 13. IR spectra in the region of C≡N stretching vibration bands at room temperature of (a) malononitrile (reactant), (b) **1a** containing malononitrile, (c) **1a** containing ethyl cyanoacetate, and (d) **1a** containing cyano-acetic acid *tert*-butyl ester. The bands marked with an asterisk indicate the C≡N stretching vibration bands due to each substrate that is not activated.

methanol at 298 K are shown in Figure 11. The adsorption isotherm showed gradual uptake to $P/P_0 = 0.9$. Conversely, the desorption isotherm did not trace the adsorption profile and decreased slightly until a sudden drop at $P/P_0 = 0.1$, with a large-range hysteresis loop. This characteristic adsorption profile shows the conversion of amorphous **1b** to the crystal **1c**. The interaction between the host framework and methanol is strong enough to transform and maintain the channel structure, so that the large hysteresis profile appears. The amount of adsorbed methanol is 3.2 molecules per 4-btapa ligand at $P/P_0 = 0.9$, which is close to that calculated from the TGA measurement for **1c**. This result also supports the proposition that the adsorbed methanol is bound to the amide groups of **1c** in a 1:1 ratio. From these results, we conclude that the amide groups on the channel surfaces function effectively and give rise to an attractive interaction with the methanol guest molecules via hydrogen bonding. The structural transformation is inspired by the interaction between the guest molecules and the host framework.

Selective Inclusion and Activation of Reactants in Selective Catalytic Reactions. Amide groups have two sites that are involved in their function in different ways. In **1a**, the −NH moiety acts as a hydrogen donor for short-chain alcohols in the channels, whereas the −C═O moiety acts as an electron donor. Recently, a study reported a PCP with base carbonyl oxygen atoms as the catalytic interaction sites on the channel wall.[4g] We also expected the −C═O moiety in the channels of **1a** to provide guest interaction sites as base sites. To confirm the selective accommodation and activation of reactants by **1a**, selective adsorption experiments were performed to identify the substrates of **1a**. The substrates chosen for the reaction were malononitrile (molecular size, 6.9 × 4.5 Å^2), ethyl cyanoacetate (10.3 × 4.5 Å^2), and cyano-acetic acid *tert*-butyl ester (10.3 × 5.8 Å^2).[22] As-synthesized **1a** was immersed in benzene containing each reagent and stirred. The powder was filtered off and dried in air, and then its ^{1}H NMR and IR spectra were acquired. The ^{1}H NMR spectra showed that **1a** adsorbs 2.9, 0.7, and 0.6 molecular stoichiometric amounts of malononitrile, ethyl cyanoacetate, and cyano-acetic acid *tert*-butyl ester per 4-btapa ligand of **1a**, respectively (Figure 12). The inclusion amount of malononitrile for **1a** was 4−5 times larger than those of the other reagents, implying that the smallest molecule, malononitrile, was most easily introduced in the channels of **1a**. From
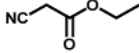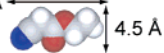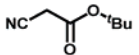
the IR spectra, only malononitrile interacted with the host **1a**. In general, when an active methylene compound interacts with part of the α-H atom, the IR band attributed to the C≡N stretching vibration shifts to a lower wavenumber and $v^s_{CN}-v^{as}_{CN}$ splitting appears.[23] The $v^s_{CN}-v^{as}_{CN}$ splitting at 2180 and 2200 cm^{-1} was observed for malononitrile in **1a**, whereas the other reagents showed only the original peak (Figure 13). Malononitrile in the channels of **1a** may interact with the −C═O moiety of the amide groups via hydrogen bonding. Unfortunately, the shift in the peak for the −C═O stretching vibration was not large because the amide groups of the original **1a** had already interacted with the guest molecules, which maintain the channels of **1a**. Therefore, it was difficult to observe the shift in the peak of the −C═O stretching band. It is worth noting that the IR spectrum of **1a** containing malononitrile shows two types of guests: one interacting with the host **1a** and the other not interacting. These ^{1}H NMR and IR results indicate that the smallest molecule, malononitrile, is selectively adsorbed and activated in the channels of **1a**.

(22) These molecular sizes are calculated based on the CPK model.

(23) Binev, I. G.; Binev, Y. I.; Stamboliyska, B. A.; Juchnovski, I. N. *J. Mol. Struct.* **1997**, *435*, 235−245.
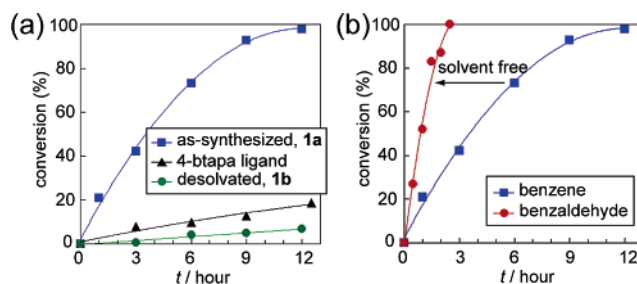
Table 2. Knoevenagel Condensation Reaction of Benzlaldehyde with Substrates, Catalyzed by **1a**

run[a]	substrate	molecular size	conversion[b] (%)
1	NC — CN	6.9 Å × 4.5 Å	98
2	NC — O (ethyl cyanoacetate)	10.3 Å × 4.5 Å	7
3	NC — O-*t*Bu	10.3 Å × 5.8 Å	0

[a] All reaction were performed with 2 mmol substrates in 10 mL of benzene using 0.1 g (0.08 mmol, 4 mol %) of the as-synthesized **1a** for 12 h. [b] Determined by ^{1}H NMR, based on starting materials.

Base Catalytic Properties of 1a. Although several studies about PCPs with acid properties have been reported,[4a,c−e,5e−f,24] studies of PCPs with base properties have been few.[4b,4g,25] To characterize the base-type properties of **1a**, a Knoevenagel condensation reaction catalyzed by **1a** was performed. The Knoevenagel reaction is well known, not only as a weak base-catalyzed model reaction but also as a reaction that generates a C−C bond.[26] However, to our knowledge, the reaction has never been reported in the context of PCP. Knoevenagel condensation reactions of benzaldehyde with each of the active methylene compounds (malononitrile, ethyl cyanoacetate, and cyano-acetic acid *tert*-butyl ester) were catalyzed by **1a**. As a result, the malononitrile was a good substrate, producing 98% conversion of the adduct, whereas the other substrates reacted negligibly (Table 2). This guest-selective reaction suggests that the reaction occurs in the channels and not on the surface of **1a**.

Only as-synthesized **1a** promoted the reaction with a good yield compared with desolvated **1b** or the 4-btapa ligand (Figure 14a). Desolvated **1b** has no channels, and the 4-btapa ligand has no free amide groups because it forms an intermolecular hydrogen bond among themselves.[10] We also checked that no reaction occurred with Cd(NO$_3$)$_2$·4H$_2$O. These results also support that the reaction occurs within the channels functionalized with the amide group of **1a**. The heterogeneity and recyclability of **1a** in the Knoevenagel condensation of benzaldehyde and malononitrile were examined. After the reaction mixture was stirred for 3 h in the presence of **1a**, **1a** was removed by filtration. After removal of **1a** from the reaction system, the reaction did not proceed further, demonstrating the

Figure 14. (a) Conversion (%) vs time (h) for Knoevenagel condensation reaction of benzaldehyde with malononitrile in benzene catalyzed as-synthesized, **1a** (blue square), desolvated, **1b** (green circle), and 4-btapa ligand (black triangle). (b) Reaction of solvent-free condition (red circle) is much faster than that in benzene solution (blue square). Each conversion was detected by ^{1}H NMR based on starting material.

catalytic activity of **1a**. The catalyst **1a** shows good recyclability. **1a** is easily isolated from the reaction suspension by filtration alone and can be reused without loss of activity. The XRPD patterns of the **1a** before and after the reactions were the same, indicating the high stability of **1a**. Even when **1a** changes its form to the amorphous state **1b**, it is easily recovered in the crystalline state by immersing it in DMF or short-chain alcohols, which cause the amorphous-to-crystalline structural transformation of the host. Therefore, this compound containing effective FOS, amide groups, can be considered to exhibit a sufficient catalytic activity with base property. Under solvent-free conditions, remarkable improvements were observed in the conversion, via Knovenagel condensation of benzaldehyde with malononitrile, catalyzed by **1a** (Figure 14b). The reaction of malononitrile (2 mmol) with liquid benzaldehyde (10 mL) was performed without benzene, and **1a** achieved a conversion to the adduct of 100% after a 2.5 h reaction time.

Conclusion

This work describes the construction of a 3D PCP containing guest-accessible amide groups and characterizes the selective inclusion of guest molecules with the structural transformation of the host. Moreover, we demonstrated a PCP that acts as a heterogeneous base catalyst based on a FOS located on its channel surfaces.

First, we successfully synthesized a 3D PCP functionalized with amide groups, {[Cd(4-btapa)$_2$(NO$_3$)$_2$]·6H$_2$O·2DMF}$_n$ (**1a**), from the reaction between Cd(NO$_3$)$_2$·4H$_2$O and a three-connector-type amide ligand (4-btapa). The amide groups of **1a** are ordered uniformly on the channel surfaces. **1a** undergoes reversible dynamic structural transformation via an amorphous state (**1b**) in response to the removal and rebinding of guest molecules. This is inspired by hydrogen bonding between the guest molecules and amide groups. We observed selective guest inclusion via the hydrogen bond, which is based on not only the size and shape of the incoming guest but also its affinity for the amide group, as demonstrated by X-ray crystallographic analysis and adsorption measurements.

Second, **1a** selectively accommodated and activated guests in its channels because of the active amide groups. As a result, the Knoevenagel condensation reaction, which is a well-known base-catalyzed model reaction, was selectively promoted in good yield. This selectivity depends on the relationship between the size of the reactants and the pore window of the host. **1a** displays a unique recoverable framework; even when **1a** changes to **1b**

(24) Vimont, A.; Goupil, J. M.; Lavalley, J. C.; Daturi, M.; Surblé, S.; Serre, C.; Millange, F.; Férey, G.; Audebrand, N. *J. Am. Chem. Soc.* **2006**, *128*, 3218−3227.

(25) Shin, D. M.; Lee, I. S.; Chung, Y. K. *Cryst. Growth Des.* **2006**, *6*, 1059−1061.

(26) (a) The number of published articles containing the keyword "Knoevenagel condensation" is shown in Figure S5. (b) Rao, P. S.; Venkataratnam, R. V. *Tetrahedron Lett.* **1991**, *132*, 5821−5822. (c) Reddy, T. I.; Varma, R. S. *Tetrahedron Lett.* **1997**, *38*, 1721−1724. (d) Rodriguez, I.; Iborra, S.; Corma, A.; Rey, F.; Jordá, J. L. *Chem. Commun.* **1999**, 593−594. (e) Harjani, J. R.; Nara, S. J.; Salunkhe, M. M. *Tetrahedron Lett.* **2002**, *43*, 1127−1130. (f) Yadav, J. S.; Reddy, B. V. S.; Basak, A. K.; Visali, B.; Narsaiah, A. V.; Nagaiah, K. *Eur. J. Org. Chem.* **2004**, 546−551. (g) Tamami, B.; Fadavi, A. *Catal. Commun.* **2005**, *6*, 747−751.

after complete guest removal, the porous crystalline structure can be easily recovered by guest adsorption and demonstrated the same catalytic activity as the initial one.

This research is particularly relevant in the context of porous solid-state chemistry in the generation of new materials with unusual properties. This result suggested that the combination of metal ions and designed organic ligand can provide PCP with FOS showing base catalytic performance. PCPs functionalized with FOS herald the next advance in porous materials that can be used as a fascinating class of adsorbents and heterogeneous catalysts.

Supporting Information Available: General experimental details and characterization data. This material is available free of charge via the Internet at http://pubs.acs.org.

JA067374Y